REPORT OF FIRE RESEARCH INSTITUTE OF JAPAN
Serial No.42 September 1976

消防研究所報告

通 巻 42 号 1976年9月

目 次

研 究

消 防 研 究 所
東 京 都 三 鷹 市

REPORT OF FIRE RESEARCH INSTITUTE OF JAPAN

Serial No. 42 September 1976

Contents –

MEMOIR

Published by
Fire Research Institute of Japan,
14-1, Nakahara 3-chome, Mitaka, Tokyo, Japan.

炭酸ナトリウム主剤のナトリウム火災消火剤の開発

要旨

守川時生

ナトリウム火災の消火用に，現在，我が国で市販されている粉末系消火剤は，主に，塩化ナトリウム主剤のものと，ナトリウム主剤のものとである。前者は，腐食性の恐れがあり，後者は消火効果，すなわち，被覆持続時間の点に問題がある。本研究は，腐食性のない炭酸ナトリウムを中心とした消火剤の改良開発に関するものである。。添加剤に種々の有機物，プラスチックを選んで，被覆効果の増強を試みた。実験は，内径4.5cmのステンレス製同筒容器の下半分を電気炉で加熱し，上半分を水分した装置で行なった。約30gのナトリウムを550℃に加熱後，燃焼させ，消火剤で燃焼ナトリウムを被覆し，その温度を保持しながら消火剤の効果の効果の観察を行なった。その結果，熱分解の際に炭化物残渣を生じ，主剤の架橋剤として作用するポリアクリロニトリルと，消火剤適用後，しばらくの間，溶融して消火剤に粘着性を与え，薬剤層のひび割れを防止するポリエチレン，ポリスチレン，または，ステアリン酸マグネシウムを添加剤として用いると，被覆は約1.5cmでも，30分間以上耐えることがわかった。その配合は，炭酸ナトリウム90%，ポリアクリロニトリル6%，および，ポリエチレンなど4%である。。

A New Sodium Carbonate-Based Extinguishant for Sodium Fires

Tokio Morikawa

Laboratory scale experiments were conducted in an attempt to improve a non-corrosive sodium fire extinguishant consisting mainly of sodium carbonate. The use of a combined additive of polyacrylonitrile and polyethylene was found to be very effective in improving the conventional sodium carbonate-based extinguishant.

Introduction

It is expected that the use of sodium in a high temperature liquid state will increase in the future when breader reactors are substantially put into practice, because sodium has a high heat transfer coefficient and a wide range of liquid temperature. High temperature liquid sodium is used isolated from air, since it can ignite even below 300°C in air[1-3]. However, it is still necessary to develop sodium fire-extinguishing methods, because sodium fires will break out if sodium leaks and is exposed to air.

In principle, sodium fires can be extinguished either by removing oxygen or by cooling the sodium. Self-sufocation, dilution of oxygen with an inert gas, and covering the surface of sodium with extinguishant powder are popular means to extinguish sodium fires. The former two are superior to the latter in that cleaning-up work is not required after the fire has been extinguished. The biggest problem with these 2 methods is that it is not easy to maintain the oxygen concentration below 5%[1,4] until the sodium has cooled down to its ignition temperature. Therefore, these 2 methods are not suitable except for limited situations.

The use of powder-type extinguishants is usually considered to be more practical. Commercially available sodium fire extinguishants of powder-type consist mainly of sodium carbonate, sodium chloride, or a mixture of sodium chloride, potassium chloride and barium chloride. The latter two have a possibility of causing a corrosion to costly austenic stainless steel equipment which is used together with sodium. The former has difficulty in maintaining its crust over the sodium surface for a long period of time. Although sodium burns much slower than oil, large sodium fires are not easy to extinguish because of the poor performance of existing extinguishants.

The present study mainly concerns attempts to improve a sodium carbonate-based extinguishant, although other inorganic materials were also tested on burning sodium.

Experimentals

The experimental apparatus, as illustrated in Fig. 1, consists of a stainless steel cylinder (4.5cm height) with a flange at half height, a cylindrical electric furnace and a temperature-controlling system. The lower half of the cylinder was placed inside the furnace while the upper half, which was cooled with running water through a copper tube, was left outside. The sodium temperature in the cylinder was controlled automatically using a sheathed chromel-alumel thermocouple (2mm dia.) inserted into the sodium down to the bottom along the cylinder wall. Sodium (32g) and extinguishant powder (24g, about 1.5cm thick) were principally used for each experiment. The cylinder was covered with a lid until the sodium temperature was raised to a given temperature (mainly 550°C). After the lid was removed, the sodium was allowed to burn for one minute. After the surface film was broken by stirring, the powder was applied on the burning sodium surface with a spoon. Then, the behavior of the powder on the sodium was observed for not more than 30 minutes.

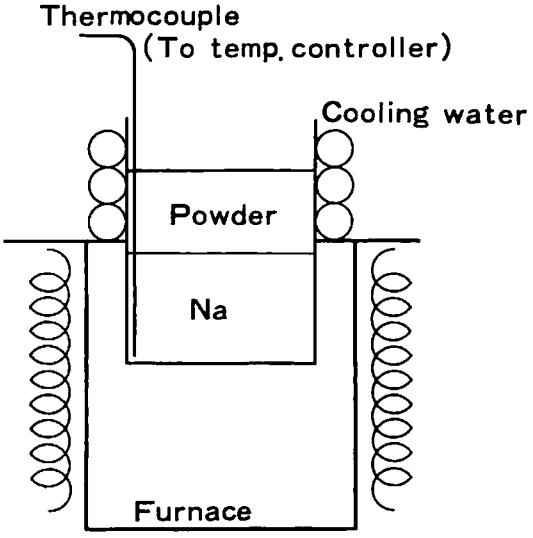

Fig. 1 Experimental apparatus

Base materials for powder mixtures were a commercial sodium carbonate-based extinguishant, Natrex (Na_2CO_3 98%, Mg-stearate 1.9%, thermocolor 0.1%) or the first grade sodium carbonate. Plastics used as additives were powdered industrial products.

Reaction of various inorganic materials with sodium was observed when a small portion of each material was put over sodium burning at 550°C.

Pyrolysis of various plastics and other organic materials as additives was conducted in a nitrogen gas flowing-quartz tube inserted into a cylindrical electric furnace. The specimen was subjected to pyrolysis at 350 or 550°C for 5 minutes, and then the residue was observed.

Results and Discussion

Behauior of various inorganic materials on sodium

The results are shown in Table 1. Except for sodium carbonate, the materials tested reacted with sodium or burned with the aid of the heat from burning sodium. Sodium carbonate was easily wetted with molten sodium and sank, although it did not react with sodium. Sand and vermiculite have been considered to be applicable to sodium fires, but they reacted violently with sodium at 500–550°C by reduction reaction.

Inorganic materials which are solids at normal temperature and which do not react with burning sodium are mainly limited to sodium carbonate, potassium carbonate, alkalin halides and some elemental substances.

Table 1 Behavior of various inorganic materials on burning sodium at 550°C

Sand	Reacted violently
Vermiculite	Reacted violently
Calcium oxide	Reacted violently
Calcium carbonate	Reacted violently
Graphite	Burned
Shirasu-ball (volcanic sand)	Reacted violently
Sodium borate anhydrate	Reacted violently
Sodium carbonate	Did not react

Pyrolysis of various organic materials

Various plastics and other organic materials were subjected to pyrolysis at 300 and 550°C in a current of nitrogen gas to screen for additives or binders for powder base materials. The results are shown in Table 2. In the pyrolysis at 550°C, polyethylene (PE), polypropylene (PP), polystyrene (PS) and polymethyl methacrylate (PM) yielded no carbonaceous residue. But at 300°C, these materials became free-flowing liquids.

Table 2 Behavior of various organic materials pyrolized under nitrogen atmosphere

	300°C	550°C (carbonaceous residue)
Polyacrylonitrile	Yielded carbonaceous residue	Yes
Polyethylene	Melted	No
Polypropylene	Melted	No
Polystyrene	Melted	No
Urethane foam	Turned brown	No
Polyvinyl chloride	Yielded carbonaceous residue producing smoke violently	Yes
Mg-stearate	Melted	Yes (a little)
Vinylon	Melted	Yes
Albumin	Yielded carbonaceous residue	Yes
Nylon-6	Melted	Yes

From the results, materials which contain nitrogen in their molecules were generally found to yield carbonaceous residue at 550°C. But polyacrylonitrile (PAN), albumin and polyvinyl chloride (PVC) were the only materials which yielded carboneceous residue at 300°C as well.

Based on these results, organic materials, as additives for extinguishants, can be divided into three categories; (1) those which melt and stay in the liquid state until they completely evaporate or decompose without yielding any carbonaceous residue (PE, PP, PS, PM, etc.), (2) those which yield carbonaceous residue immediately after melting (PAN, albumin, PVC, etc.) and (3) those which are a combination of (1) and (2) (Nylon-6, urethane resin, etc.)

Sodium fire extinguishment

Some inorganic compounds and elemental substances are possible sodium fire extinguishants for powder types now being used. If corrosive halogen salts, high density metals, oxygen-reacting carbon black and hygroscopic compounds are eliminated, sodium carbonate will offer the greatest possibility as an effective sodium fire extinguishant base. The commercial sodium carbonate-based extinguishant, Natrex, (hereafter NX) or the first grade sodium carbonate combined with one to four additives, mostly organic materials listed in Table 2, was applied over sodium burning at 550°C. The results are shown in Table 3.

Table 3 Effect of various materials on the extinguishment of sodium fire at 550°C

Test No.	Composition		Remarks
1	NX*	24.0g	Cracked and fell in the central area, then reignited after 10 min.
2	NX Polyethylene (PE)	23.0 1.0	Sodium surfaced in the central area after 14 min. and then reignited.
3	NX PE	22.0 2.0	Sodium surfaced after 18 min. and then reignited.
4	NX Polypropylene (PP)	23.0 1.0	Sodium surfaced after 14 min. and then reignited.
5	NX PP	22.0 2.0	Slightly subsided after 4 min., sodium surfaced after 11 min. and reignited.
6	NX Polyester	23.0 1.0	Sodium surfaced after 11 min. and then reignited.
7	NX Polyester	22.0 2.0	Sodium surfaced after 10.5 min. and then reignited.
8	NX Nylon-6	23.0 1.0	Sodium surfaced after 17 min. and then reignited.
9	NX Nylon-6	22.0 2.0	Sodium surfaced after 17.5 min. and then reignited.
10	NX Mg-stearate	23.0 1.0	Sodium surfaced after 16 min. and then reignited.

Test No.	Composition		Remarks
11	NX Mg-stearate	22.0 2.0	Sodium surfaced after 18.5 min. and then reignited.
12	NX Urethane foam	23.0 1.0	Sodium surfaced after 17 min. and then reignited.
13	NX Urethane foam	22.0 2.0	Sodium surfaced after 19 min. and then reignited.
14	NX Albumine	23.0 1.0	Cracked in the central area after 4 min; fell and sodium reignited after 12 min.
15	NX Polystyrene (PS)	23.0 1.0	Sodium surfaced after 10 min. and then reignited.
16	NX PS	22.0 2.0	Sodium surfaced at the edge after 24 min. and then reignited.
17	NX Polyacrylonitrile (PAN)	23.0 1.0	Cracked and subsided in the central area, and then sodium reignited after 10 min.
18	NX PAN	22.0 2.0	Cracked in the central area and then sodium reignited after 10 min.
19	NX PAN PE	22.0 1.0 1.0	Sodium surfaced in the central area after 22.5 min. and reignited.
20	NX PAN PE	22.0 1.5 0.5	Cracked after 5 min., subsided after 7 min. then sodium reignited.
21	NX PAN PE	22.0 1.5 1.0	no reignition after 30 min.
22	Na_2CO_3 PAN PE	22.0 1.5 1.0	no reignition after 30 min.
23	NX PAN Mg-stearate	22.0 1.5 1.0	no reignition after 30 min.
24	NX PAN PS	22.0 1.5 1.0	no reignition after 30 min.
25	NX Albumine PE	22.0 1.5 1.0	Sodium surfaced after 16.5 min. and reignited.
26	NX Albumine PE	22.0 1.5 1.0	Sodium surfaced in the central area after 24 min. and reignited.
27	NX PAN PE	22.0 1.0 1.0	Contracted and subsided in the central area, before sodium reignited after 14.5 min.

Test No.	Composition		Remarks
28	NX	22.0	Cracked in the central area after 7 min; full and sodium reignited after 8 min.
	$Na_2B_4O_7$	2.0	
29	NX	22.0	Slightly subsided with the contraction. No reignition.
	PAN	1.0	
	PE	1.0	
	$Na_2B_4O_7$	1.0	
30	NX	22.0	Fell in the central area after 7 min. and then sodium reignited.
	PAN	1.0	
	$Na_2B_4O_7$	1.0	
31	NX	22.0	Fell in the central area after 28 min. and then sodium reignited. After the cooling-off, a cavity was observed.
	PAN	1.0	
	$Na_2B_4O_7$	2.0	
32	NX	22.0	The half was applied and the rest was applied after 6.5 min. when sodium reignited. Sodium reignited again after 29 min.
	PAN	1.0	
	PE	1.0	
33	NX**	24.0	no reignition after 30 min.

* Natrex (Na_2CO_3 98%, Mg-stearate 1.9%, Thermocolor 0.1%)
** Mytex (NaCl 86%, $CS(NH_2)_2$ 3%, $Na_2B_4O_7$ 3%, $MgCO_3$ 3%, Mg-stearate 3%, SiO_2 1.95%, Color 0.05%)

In the preliminary experiments, the temperature of the cylinder wall above the sodium surface level was so high due to the heat transfer from the furnace that it affected the performance of the agents. In the actual experiments, the upper half of the cylinder wall was cooled to avoid the overheating of the wall, because in actual fires this part of the wall is lower in temperature than the burning sodium.

For the temperature measurement and control, only one thermocouple was used on the assumption that the temperature distribution in the sodium was uniform[5].

The layer of NX contracted and cracked, as it was heated. A part of the layer fell and the sodium became exposed to air 10 minutes after the application of NX (Photo 1). It was also observed that sodium came up to the surface due to capillary action. The plastics of category (2) made the sodium wet and fluid and presented the capillary phenomenon. The endothermic pyrolysis reaction of the additives presumably contributed to the delayed ignition of sodium. When the pyrolysis was almost completed, sodium came to the surface and began to burn. Therefore, the effect of plastics in category (2) does not last long. During this process, there was no subsidence in the central part, because there was no contraction. PAN and albumin had no effect on making sodium carbonate wet and fluid. When the carbonization of these additives proceeded from the edge to the center, contraction of a layer of the agent occurred. The contraction resulted in a crack in the layer because of the lack of wetting and fluidizing effect of these additives.

The use of a combined additive of PAN and either PE, PS or Mg-stearate improved the effect of the agent sufficient to maintain a cover over the 550°C sodium for 30 minutes, as shown in No. 21, 23 and 24 of Table 3. In these experiments, NX was used as a base material,

but a mixture of the first grade Na_2CO_3, PAN and PE (No. 22) was found to be as effective as formulations, No. 21, 23 and 24. The result of No. 2 after 30 minutes is shown in Photo 2. It is indicated that ordinary sodium carbonate powder can be used as a base material. As for No. 21–24, tests were repeated to insure the reproducibility.

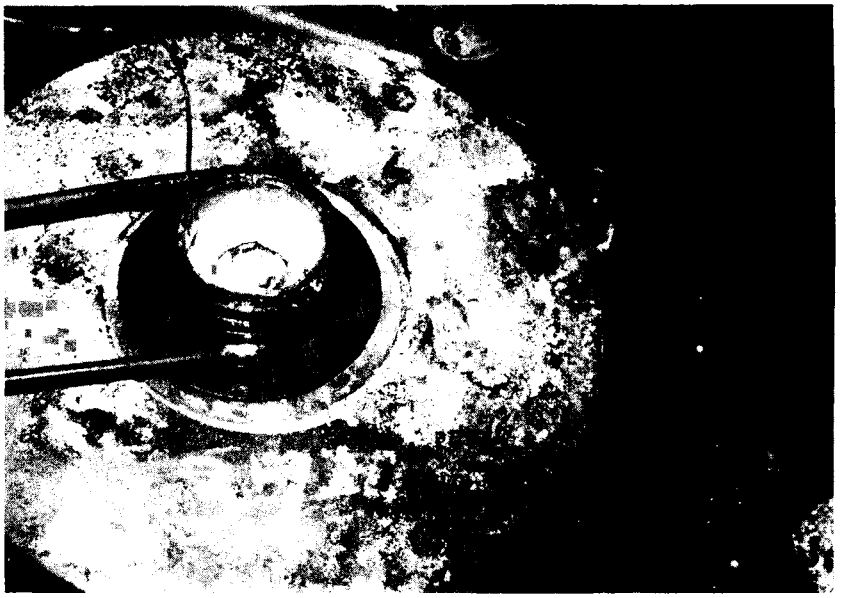

Photo 1 Test No. 1
10 min. after the application of the agent.

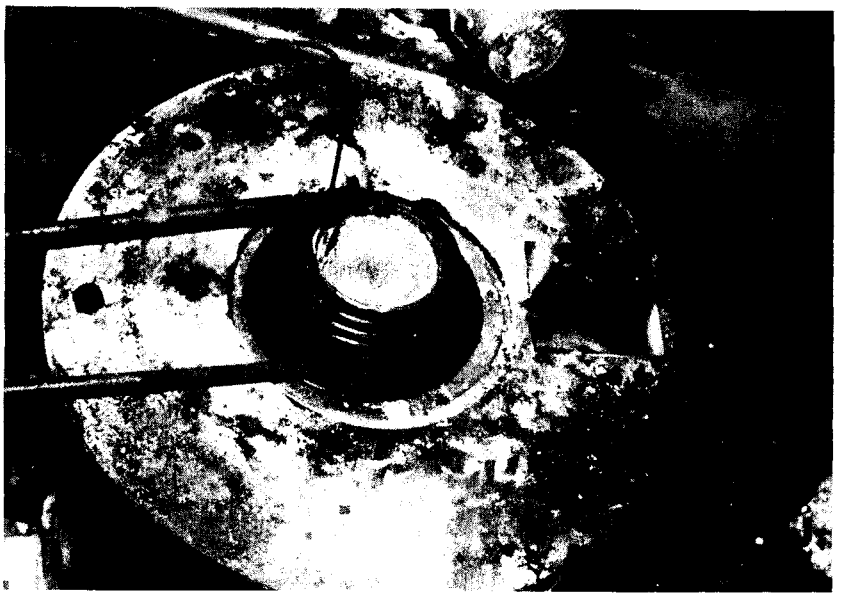

Photo 2 Test No. 22
30 min after the application of the agent.

In principle, it is believed that the materials at category (1) prevent the layer of the agent from developing a crack until the materials of category (2) turn into a carbonaceous material which then functions as a binder for the agent.

In a practical case, Mg-stearate would cause trouble with transportation through a pipe when used in a great quantity as contained in the formulation No. 23. Polystyrene would evolve a great amount of smoke and soot, if it caught fire. Therefore, the formulation, No. 23, with a small amount of Mg-stearate added as a lubricant as well as water repellent will be the most practical agent.

Thermal decomposition products of additives flamed a little with the application of a small amount of agent or in the early stage of the application. But, when the entire surface of the sodium was covered with the agent, the flaming stopped.

The use of albumin in place of PAN in the formulation No. 21 was not as effective. Nylon-6 of the category (3) was used together with PAN, but formulations containing nylon-6 were not as effective as formulations, No. 21–24.

A commercial sodium chloride-base extinguishant (Mytex) was found to be as effective as the above-mentioned formulations. This possibly corrosive extinguishant was tested only for the purpose of comparison.

Since it has been reported that calcium carbonate has been used as a base material[7], it was tested in place of sodium carbonate. A mixture of calcium carbonate and PAN succeeded in suppressing a sodium fire of 500°C, but reacted with sodium at 550°C, as expected from the results in Table 1.

The formulation in No. 19 was used in 2 portions for Test No. 32. The first half was applied by the standard procedure, and the second half was applied after the reignition of sodium occurred. Total time of final reignition from the first application was 29 minutes compared to a reignition time of only 22.5 minutes in Test No. 19. This indicates that divided applications are more effective than one application of the same amount of extinguishant. Under actual conditions, this will also be more economical, since excessive amount of the extinguishant after the fire has been suppressed, is not very effective.

In order to determine if a combination of powder and oxygen-depleted atmosphere works better in suppressing a sodium fire, NX was applied to sodium burning at 500°C in an oxygen atmosphere of 10% diluted with nitrogen gas. It was found that the oxygen dilution to this extent had little effect on controlling the sodium fire.

The powder mixtures containing organic additives has densities much higher than that of high temperature sodium, but did not sink into the sodium. Even though the reason has not been clarified, the molten or carbonized organic additives must have played an important role in preventing the mixture from sinking into the sodium. There is also an indication that the density of base materials does not necessarily have to be lower than that of sodium.

The experimental conditions used in this evaluation were considered to be very severe in that sodium temperature was maintained at 550°C for 30 minutes and only about 1.5cm thickness of powder was used. Although the surface area and depth of sodium used were small in scale, it can be assumed that the effect of extinguishant will be the same in larger scale

sodium fires, because the burning characteristics of sodium is not so dependent upon area and depth as in the case of oil fires. But it will still be necessary to further study the effectiveness of the formulations mentioned above in larger scale tests because of the usual problems encountered in scaling.

Conclusion

Preliminary experiments proved that sodium carbonate was one of the most suitable materials for use as a non-corrosive sodium fire extinguishant base. However, sodium carbonate could not be used alone, because it got wet easily and sank into the molten sodium. A mixture of sodium carbonate 90%, PAN 6% and either PE, PS or Mg-stearate 4% proved to be a satisfactory sodium fire extinguishant. It is believed that molten PE, PS or Mg-stearate makes the mixture wet and fluid, while the carbonaceous material from PAN acts as a binder for the powder of the base material, sodium carbonate.

In the practical approach, while PAN and PE should be used as the major additives, Mg-stearate could also be added to make the extinguishant more fluid as well as act as a water-repellant.

References

1. J.D. Gracie, J.J. Droher, NAA-SR-4383
2. K. Akita, S. Yamashika, Report of Fire Research Institute of Japan, No. 24 (1964)
3. T. Kitagawa et al., J. Japan Society for Safety Engineering, Vol. 7 No. 1 (1968)
4. JAERI-memo 3811 (1969)
5. Japan PNC, SJ278 75-01
6. R.K. Hilliard et al., U.S. Position Paper – Sodium Combustion & Its Extinguishment-Techniques, presented at Meeting on Sodium Combustion & Its Extinguishment-Techniques & Technology.

煙中の視程について
（第５報　避難時の許容煙濃度について）

（概　要）

神　忠久

（昭和51年５月19日受理）

煙の中での歩行実験から避難時の許容煙濃度を求めてみた．この値は，避難時に必要とされている見透し距離が確保できる煙濃度の値とおおよその一致をみた。ただ，許容煙濃度は，建物内の熱知度や目，のどへの刺激の度合，さらには避難路中の障害物の有無とか，何かを捜し求める場合とかによりかなり異なる。したがって，これらのことがらを総合的に考慮すると避難時の許容煙濃度は，建物内熟知者に対しては減光係数で約0.4/m～1.2/m，デパートや地下街にいる不特定者に対しては減光係数で約0.1/m～0.3/m程度と考えられる。

Visibility through Fire Smoke (Part 5 Allowable Smoke Density for Escape from Fire)

by Tadahisa Jin

(Received May 19, 1976)

With a view to determining the allowable smoke density for escaping from a building in fire, walking speed in smoke under various conditions was studied. The allowable density values deduced from the walking speed measurements agree approximately with those given on the basis of minimum visibility for safe escaping. The allowable smoke density will considerably be affected by a) degree of familiarity with the inside of building, b) irritation caused by the smoke, c) existence of obstacles in escape route, and so on.

1. Introduction

High-rise building fires have claimed steadily increasing number of victims in recent years, and it is generally agreed that most of the toll has been demanded by the smoke. In view of this fact, study on human behaviors in smoke is of importance to introduce any effective guidance for fire escaping. It is, however, very difficult to observe human behavior experimentally under a panic condition or a close to one condition because such experiments are always attended with danger of life. Accordingly very few attempts have been made so far.

This paper includes considerations on the factors that hamper human activities in smoke and also in the allowable smoke density in the event of escape from a fire. These considerations were done on the basis of the results of a series of experiments on the speed at which people can walk in the smoke under various conditions.

2. Test Equipments and Procedures

The test equipments are shown in Fig. 1. A 20-meter long corridor was filled with smoke equivalent in density to that which would be produced at an early stage of a fire and the subjects were instructed to walk into the corridor from one end. The purpose of this experiment is to find the distance in meter at which the lighted FIRE EXIT sign placed at the other end of the corridor becomes visible to each subject [1], and at the same time the speed at which each subject managed to walk through the smoke-obscured corridor was recorded. Each subject went into the smoke holding one end of a PVC-coated electric wire in his hand. The other end of the wire was wound around a big reel, whose rotational speed was used to monitor and record his walking speed. The subjects, all male whose ages and visual acuities are listed in

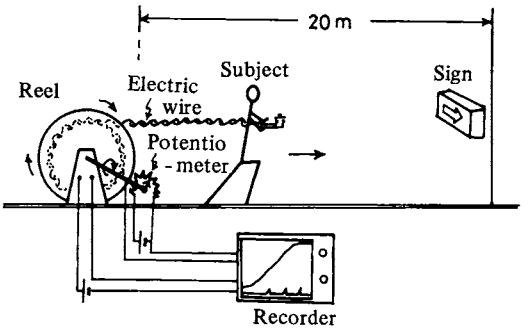

Fig. 1 Arrangements for measuring walking speed in fire smoke.

Table 1, were given no air mask and had been held in a normally lighted room before entering the test site.

Table 1 Subjects' visual acuity and age

Subject	Visual acuity		Age
	(Right)	(Left)	
A	0.8	0.5	23
B	1.0	1.5	36
C	0.8	0.8	37
D	0.8	1.0	28
E	1.0	1.0	23
F	1.0	1.2	26
G	0.8	0.5	30
H	1.2	1.2	30
I	1.0	1.2	26
G	1.0	1.2	31

Observation was also made to determine how various degrees of irritation in the throat and eye caused by the smoke affect the subjects' walking speeds. Highly irritant white smoke was produced by burning wood cribs with narrow spacing between sticks and less irritant black smoke was produced by burning kerosene.

Also made was a comparative observation of walking speeds in lighted corridor (average 80 lx at floor level) and those under power failure condition (actually, light ranging from 0.1 to 0.5 lx was present due to the EXIT sign and leaks from the smoke density meters described below).

In order to measure the density of smoke, two light-transmittance type smoke density meters with 4-meter light path and one such meter with 1-meter light path were placed at appropriate horizontal intervals 1.5m above the corridor floor.

3. Results and Considerations

The relation between the smoke density (extinction coefficient) and the walking speed is

plotted in Fig. 2. It shows that the latter decreases as the former increases. It can well be

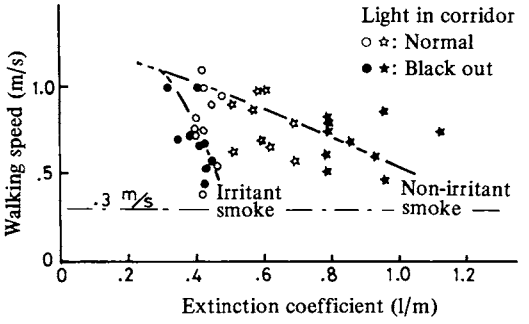

Fig. 2 Effects of smoke density and irritation on walking speed.

concluded that visibility of the wall or floor which deteriorates as the smoke becomes thicker forces the subjects to slow down. Such tendency is also observed in Watanabe's experiment[2] (see Fig. 3). As the smoke density is further increased, the condition becomes very much like

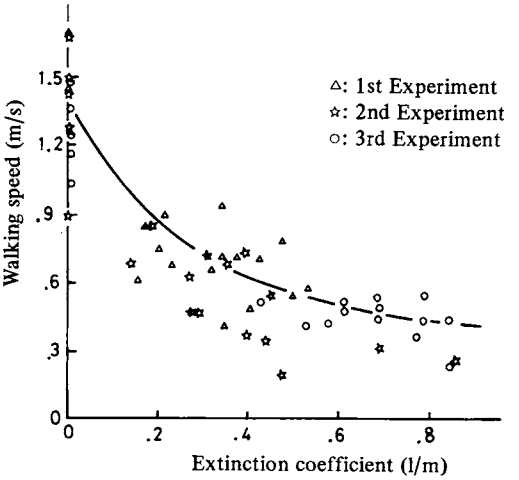

Fig. 3 Walking speed in smoke of fireman with air mask, plain work suit, and hand light. To simulate obstacles, logs about 15cm in diameter were placed across the path on the floor 3m apart from each other. (Y. Watanabe)

walking in darkness (0.3–0.7m/s)[3], under which the subjects tend to go on with their hands touching the wall, and their walking speed becomes more dependent on the wall configuration or on the way each subject takes advantage of it rather than on the smoke density itself.

The walking speed is also dependent on degrees of irritation caused by the smoke of given density as shown in Fig. 2. When the irritation has reached a certain level, the walking speed

rapidly drops because, with such acute irritation, tears run so heavily that the subject can no longer walk straight and begins to go zigzag or walk along the wall. In a thin smoke density, however, the irritation is less offensive and the walking speeds measured are much the same as those measured under non-irritant smokes.

The relation between the walking speed and the visibility of the EXIT sign given as threshold distance at which the sign is legible to each subject is shown in Fig. 4. It shows that

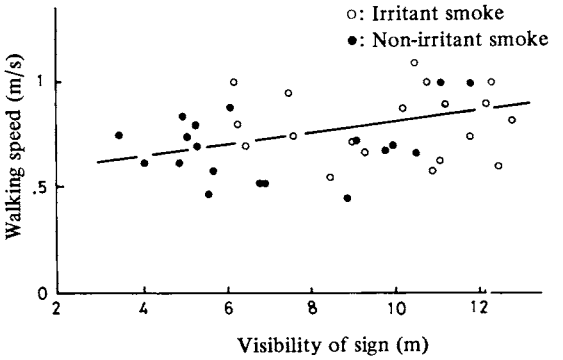

Fig. 4 Relation between walking speed and visibility at legible threshold of FIRE EXIT sign.

the walking speed slowed down as the visibility deteriorates and that its speed is more a function of visibility range than that of the degree of irritation caused by the smoke.

Occasionally the subjects would temporarily stop to look for or read the EXIT sign but, throughout this series of experiments, their walking speeds are given in the average over the entire length of the corridor including such temporary stops.

Although it was attempted to compare the walking speeds in lighted corridor with those in the corridor with no light source except for the EXIT sign, no difference could be observed between them as Fig. 2 indicates. This experiment suggests that a poor illumination in the corridor may not substantially affect the escaping for persons familiar with the building, while the necessary illuminating condition for strangers is hard to determine from the date obtained so far.

The walking speed in smoke is also depended on the degree of familiarity with the inside of building. However, Horiuchi's experiment[4] suggests that the walking speed of strangers who is conducted by familiar people with inside of building are quickly. In his experiment, each escaping group is made of five to seven persons. The walking speed of the escaping groups in corridor are shown in Fig. 5. The walking speed in this experiment is about 1.5 times than other experiments. The main reasons are the following; (1) the leader is familiar with the inside of building, (2) obstacles exit in the escape route in case of Watanabe's experiment, (3) the escaper is searching something on the way in case of author's experiment.

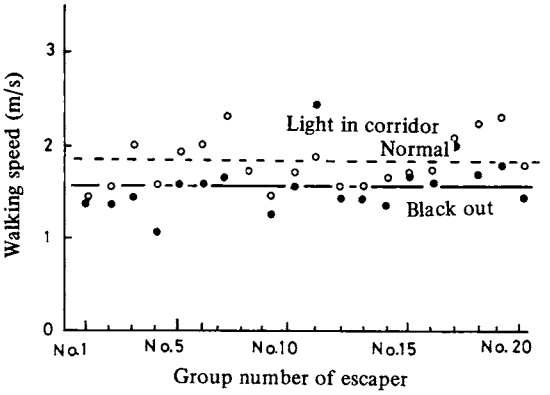

Fig. 5 Walking speed of group-escape in corridor. Each group is made of five to seven persons. Smoke density is about 0.6/m in extinction coefficient produced by smoke bomb. (S. Horiuchi)

The main factor that slows down walking speed as the smoke density increases is the deterioration of visibility by the smoke. People escaping in the smoke begin to feel uneasy when the visibility is reduced to a certain range and confusion would result especially at places such as department stores or underground arcades where a large number of strangers gather. The minimum visibility required for safe escaping, however, has not yet to be determined.

In Table 2 are listed some of the values of such visibility or allowable smoke density in fire

Table 2 Values of visibility and allowable smoke density for fire safe escape proposed by fire researchers.

Proposer	Visibility	Smoke density (Extinction coefficient)
Kawagoe[5]	20 m	0.1/m
Togawa[6]	–	0.4/m
Kingman[7]	4 ft (1.2 m)	–
Rasbash[8]	15 ft (4.5 m)	–
Los Angeles Fire Department[9]	45 ft (13.5 m)	–
Shern[10]	–	0.2/m

escaping proposed by researchers who have conducted many fire experiments. Wide variation in the proposed values are probably due to difference in places and assumed composition of the group escaping from fire. Analysis of the informations contained in this table suggests that 15 to 20-meter visibility is necessary for safe escaping at places such as department stores or underground arcades which accommodate a large number of strangers; while 3 to 5-meter visibility might be sufficient in buildings intended to accommodate a relatively small number of people and if visitors are familiar with the inner configuration of the buildings.

Maximum smoke densities (maximum allowable levels of density) that would provide for

Table 3 Minimum visibility and calculated allowable smoke density for safe escaping.

Degree of familiarity with building	Visibility	Smoke density (Extinction coefficient)
Unfamilier	15 – 20 m	0.1/m
Familier	3 – 5 m	0.4 – 0.7/m

those proposed visibility are listed in the third column of Table 3. It should be noted that people who are unfamiliar with the inside of the building need several times as much visibility for safe escaping as that needed by those who are familiar with it.

The relationship between the visibility and the smoke density as stated in terms of extinction coefficient can be expressed by the following equation [11].

$$\text{Visibility (m)} \times \text{Extinction Coefficient (1/m)} \fallingdotseq 2$$

Assuming that the smoke density that slows the average walking speed to 0.3m/s (the speed in darkness shown by a horizontal broken line in Fig. 2) is the maximum density under which people familiar with the building can safely escape, this density level is equivalent to approximately 0.5/m–1.2/m in extinction coefficient. Assuming again that a low density level at which irritancy of the smoke does not affect the walking speed is the maximum allowable smoke density for safe escape of strangers, such density is equivalent to about 0.2/m–0.3/m in extinction coefficient. These values substantially coincide with the allowable smoke densities listed in Table 3.

In one experiment in which the author himself played the subject, he managed to withstand a non-irritant smoke from kerosene equivalent to 1.8/m in extinction coefficient for approximately five minutes without air mask. Such high density, however, is not applicable of course when considering safe escape for the public.

Interesting datum were published recently by D.J. Rasbash[12]. Visual ranges of various degrees were produced by filling the test site with smoke of various density levels and his subjects were instructed to walk into the smoke to find how many of them would give up going

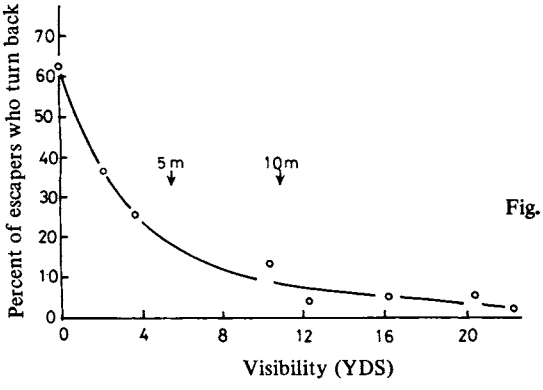

Fig. 6 Effect of visibility on percentage of people who try to move through smoke at fire and turn back. (D.J. Rasbash)

forward and return midway at given visual ranges. The results are quoted in Fig. 6. It shows about 20 percent of the subjects returned midway when the visual range was 5m, and 10 percent returned when the range was increased to 10m. Based on this experiment, Rasbash proposes 10m as the visual range required for safe fire escaping. The smoke density with this visibility is about 0.2/m in extinction coefficient, which approximately agrees with the previously discussed density level allowable for strangers.

4. Conclusion

The allowable smoke densities for safe escape are affected by the degree of familiarity with the inside of the building and irritation caused by the smoke as well. The maximum smoke density for safe escape of people who are familiar with the building is equivalent to approximately 0.4/m–1.2/m in extinction coefficient, while that for safe escape of people who are unfamiliar with it is equivalent to about 0.1/m–0.3/m in extinction coefficient.

Experiments to find allowable smoke density in fire escaping are not easy to perform because of possible danger to the life of subjects. This implies an accumulation of vast amount of data through numerous experiments simulating a variety of conditions of fires is required before this question can be satisfactorily answered. The author hopes the present work may contribute something to the effort in that direction.

5. Acknowledgment

The author would like to thank Mr. Y. Kumano, Director of the Fire Research Institute, for his constant support and interest in this work.

Reference

1) T. Jin: Bull. of Japanese Assoc. of Fire Sci. & Eng., 22, 1-2, 11, (1972)
2) Y. Watanabe: Report of Fire Research Institute of Japan, 37, 15, (1973)
3) K. Togawa: Kenchiku Sekkei Shiryo shusei, 6, 378, Maruzen, (1969)
4) S. Horiuchi, M. Murozaki, T. Jin: Annual Meeting of Architectural Institute of Japan (Planning P. 581, 1974)
5) K. Kawagoe, H. Saito: J. of Japan Soc. for Safety Eng., 6, 2, 108, (1967)
6) K. Togawa: Unpublished
7) F.E.T. Kingman: J. Appl. Chem., 3, 463, (1953)
8) D.J. Rasbash: Fire, 59, 735, 175, (1966)
9) Los Angeles Fire Department: Operation School Burning, (1961)
10) J.H. Shrn: 69th Annual Meeting of the ASTM, (1966)
11) T. Jin: Report of Fire Research Institute of Japan, 33, 31, (1971)
12) D.J. Rasbash: International Seminar on Automatic fire Detection (Aachen, West Germany, 1975)

空気中における高分子の等温熱分解による重量減少速度　(第一報)
セルロース，レーヨン，ポリエステル繊維

斉藤　直，箭内英治

(昭和51年5月31日受理)

1. 諸言

合成高分子が日用品，建築材料および化学繊維として広範に日常生活に取入れられるにつれ，火災時に，これらの合成高分子を原料とする製品から発生する煙や有毒ガスによる危険性が指摘され，その検討がなされてきている。[1-3)]

煙や有毒ガスによる建築材料，日用品または衣類に用いられている高分子物質の火災時における危険性は，それらの物質の熱分解による重量減少速度の大きさとも密度に関係する。[4,5)]* すなわち，煙や有毒ガスによる危険性は，それらの総発生量よりも発生速度に大きく依存すると考えられるからである。[6)]

しかし，有毒ガスによる危険性を評価する場合の基礎となる燃焼生成ガスの分析的研究の多くにおいては，試料の重量減少の測定が行なわれていない。このため，各試料から発生する有毒ガスの発生速度について知見が得られず，危険性を評価するための重要な手がかりを失っていることになる。

また，従来の研究では，試料の加熱方法として，一定の温度に加熱された炉に試料を導入する方法が多くとられている。この方法では，試料が炉温度に達する以前に試料の分解が進んでしまったり，空気などの酸化性の雰囲気中では，試料の発熱のため試料温度を一定に保つことができないことがある。このような場合には，重量減少の測定が行われていても，得られた結果の速度論的取扱が困難なうえに，相互に比較することにさえ疑問が残る。したがって，煙や有毒ガスの発生による火災時の高分子材料の危険性を，材料の重量減少速度の大きさも考慮して評価するためには，試料温度を一定にして熱分解を行い，重量減少速度を求めるのが適切である。

この報告では，試料間で比較できる重量減少速度を得るための等温熱分解装置の概要と，その装置を用いて空気気流中，350～550℃でのセルロース，レーヨンおよびポリエステル繊維について測定した重量減少速度について述べ，さらに，同様の試料を空気気流中で昇温法により熱分解を行い，得られた熱量曲線から予想される重量減少速度と比較した結果についても述べる。

2. 測定

2．1　装置

試料が顕著に反応する高温領域において，従来の方法による等温熱分解が困難であったのは，加熱炉の熱容量が大きく，試料を目的の温度まで急速に昇温することができなかったことと，試料の反応による吸発熱，特に空気などの酸化性の雰囲気中においては酸化反応による大きな発熱のため，試料温度を一定に保つことができなかったことによる。しかし，最近開発された赤外線加熱炉は熱容量が小さく，昇温冷却が従来の円筒状の電気炉に比べて極めて短時間でできるので，著

*) 燃焼速度としているものもあるが，正確には重量減少速度とすべきである。

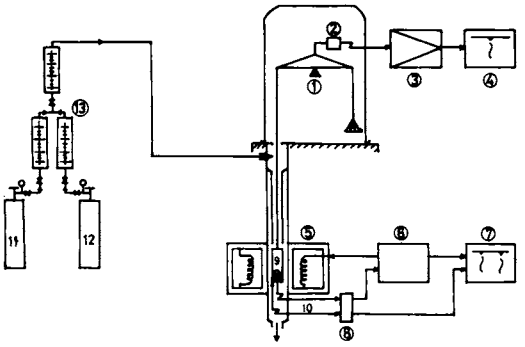

Fig. 1 Schematic diagram of isothermal decomposition apparatus.
1. BALANCE 2. LOAD CELL 3. DYNAMIC STRAIN AMPRIFIER 4, 7. RECORDERS 5. INFRARED IMAGE FURNACE 6. PID THERMAL CONTROLLER 8. COLD JUNCTION 9. CELL 10. THERMOCOUPLES 11, 12. DRY AIR AND NITROGEN 13. FLOW CONTROLLER

者らは，加熱炉として赤外線瞬間加熱装置（真空理工K.K.製RH－L－E25／HPC－5000－1021）を採用することにした。

試料の重量変化は化学天秤に荷重変換器（共和電業K.K.製120T－5B）を取付け，動ひずみ計（共和電業K.K.製DPM－6E）を用いて測定した。試料温度は線径0.3㎜の白金－白金（13%）ロジウム熱電対を用いた。この熱電対は赤外線瞬間加熱装置の制御用熱電対を兼ねた。炉の動作を監視するため，セルの直下にもう一つの前述と同様の熱電対を置いた。熱分解炉管と試料セルは，透明石英ガラスで作製した。炉管の外径は30㎜で，上部より空気を導入し底部より排出できるようにした。試料温度の測定は，セルの底部中央に熱電対を入れて行った。

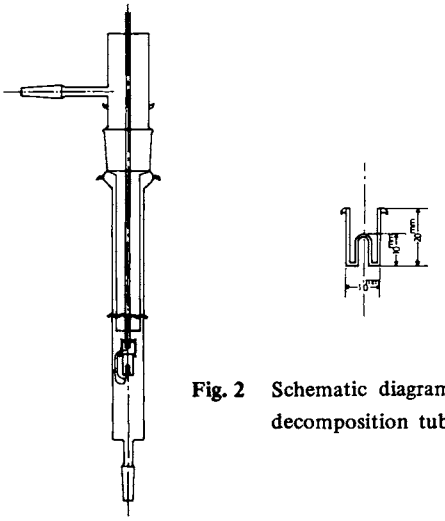

Fig. 2 Schematic diagrams of decomposition tube and cell.

乾燥空気と酸素濃度調整用の窒素は，市販のものを使用した。圧力調整器で減圧したのちダイヤフラム式流量調整弁を用いて空気および窒素流量を調節した。流量は1.2 l/min. とした。

測定装置の概略を**Fig. 1** に，熱分解炉管とセルの形状は**Fig. 2** に示した。

2．2 試料

測定に用いた試料のうち，セルロースは市販のセルロース粉末（東洋沪紙K.K.製，300メッシュ以上）を用いた。レーヨン，ポリエステル繊維は日本工業規格染色堅ろう度試験用添付白布（JIS L0803-1965）を粉末状にして用いた。試料は気乾状態のものを用い，乾燥は行わなかった。各試料の水分を昇温法による熱重量曲線から求めた結果，セルロース6%，レーヨン11%であり，ポリエステル繊維では認められなかった。

2．3 測定

等温熱分解実験の各回の測定に用いた試料量を50mgとした。赤外線瞬間加熱装置の比例－微分－積分制御の大きさを，試料温度が室温から測定温度に15秒以内に達するように調整した。試料の熱分解による重量減少速度の最大値が，加熱開始後15秒以内に現われる事のない様に加熱温度を選んだ。この実験で使用した赤外線瞬間加熱装置の温度設定ダイヤルがアナログ型のため，同一温度をくり返し設定することによる誤差は±2℃であった。

等温熱分解の場合の重量減少曲線を，同じ温度での測定を5ないし6回くり返し，それらの平均として求めた。重量減少速度は，このようにして得た重量減少曲線を数値微分することにより求められた。数値微分には3点公式を用いた。

昇温法による熱重量曲線の測定に用いた熱天秤は真空理工K.K.製TGD－3000である。試料セルには透明石英製のものを用い，試料量は10mgとした。昇温速度を10℃／min.，空気流量を50ml／min.として測定を行った。

3. 結果

3．1 等温熱分解による重量減少

酸素濃度21%の空気気流中で，350～550℃の温度範囲内で加熱した場合のセルロース，レーヨン，ポリエステル繊維の重量減少曲線を，加熱温度とともに **Figs. 3～5** に示す。重量減少曲線の初期の小さな減少量の割合は，セルロース 6.5 %，レーヨン12.5%，ポリエステル繊維 1.5%であった。**Figs. 6～8** には，それぞれの試料の重量減少速度と残重量との関係を加熱温度ごとに示した。ただし，上述の小さな重量減少の部分を除いた。

セルロース，レーヨンの重量減少速度と残重量の関係は，放物線状の単純なものであったが，ポリエステル繊維のそれは分解初期に小さな肩があり，また後期には緩くすそを引くなど単純ではなかった。

流入空気の酸素濃度を15%に減少させたときの影響をセルロース，ポリエステル繊維について調べたが，酸素濃度21%の場合の重量減少の様子と大差なかった。

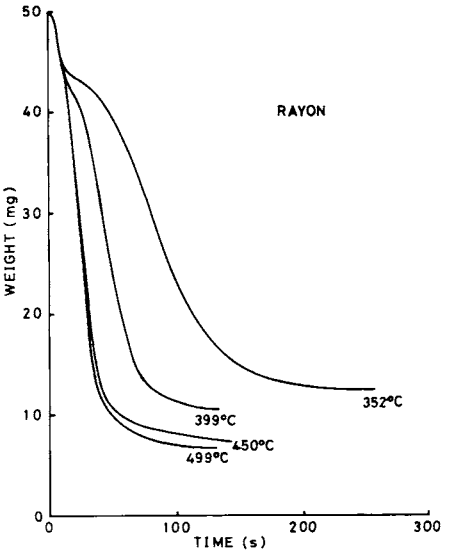

Fig. 4 Weight remaining of rayon pyrolyzed in air flow in temperature range 352–499°C.

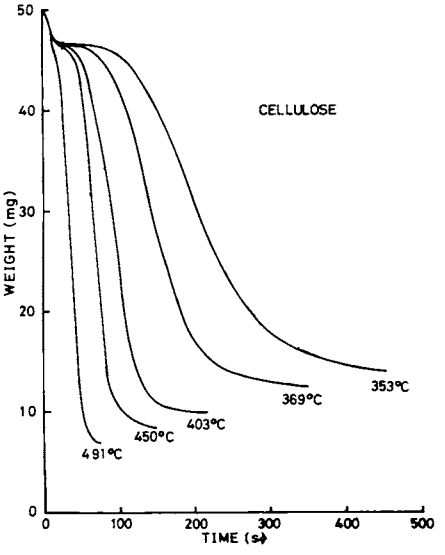

Fig. 3 Weight remaining of cellulose pyrolyzed in air flow in temperature range 353–491°C.

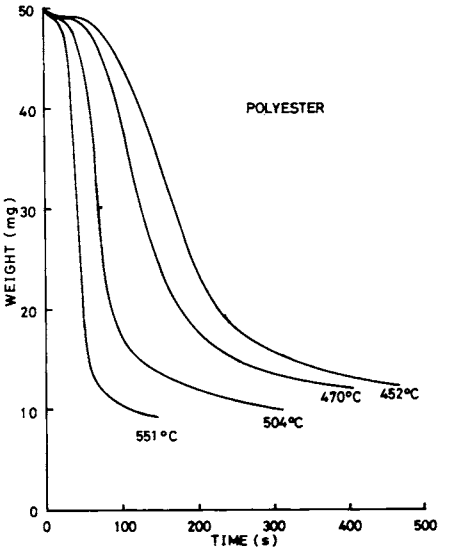

Fig. 5 Weight remaining of polyester fiber pyrolyzed in air flow in temperature range 452–551°C.

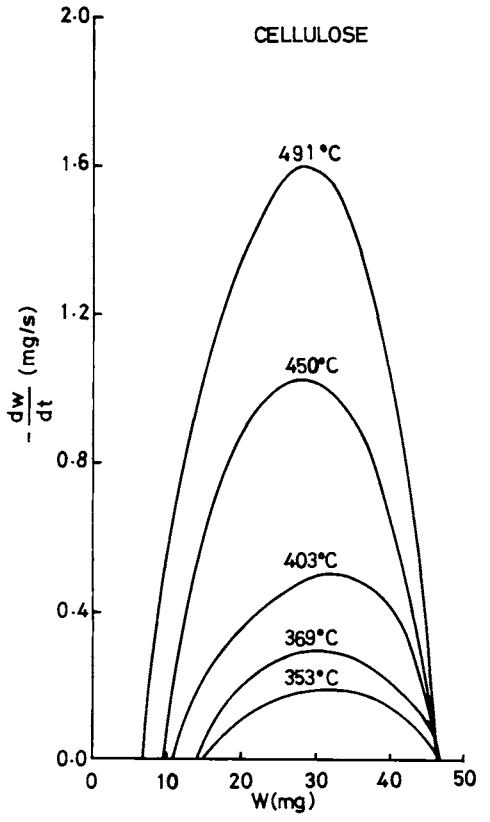

Fig. 6 Relation between weight loss rate (-dw/dt) and weight remaining (w) of cellulose.

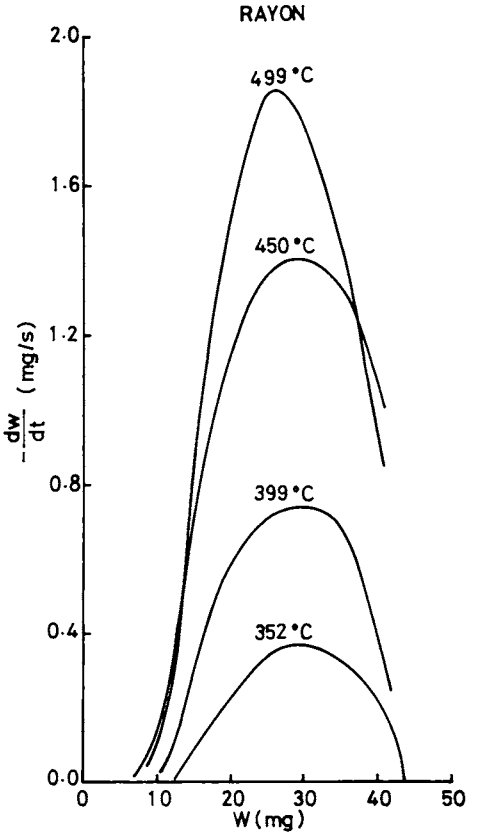

Fig. 7 Relation between weight loss rate (-dw/dt) and weight remaining (w) of rayon.

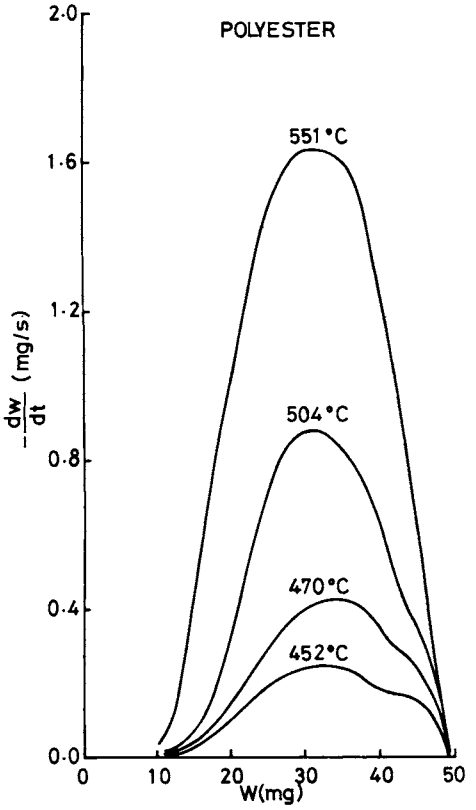

Fig. 8 Relation between weight loss rate (-dw/dt) and weight remaining (w) of polyester fiber.

3．2 昇温法熱分解による熱重量曲線

等温法で用いたものと同様の試料について，酸素濃度21%の空気気流中で測定した熱重量曲線を**Fig. 9**に示す。試料の水分の蒸発による重量減少の部分をのぞくと，空気気流中における各試料の熱重量曲線は，熱分解による重量減少の部分と残渣の燃焼による部分の二段に分かれた。熱分解による減少量が占める割合はセルロース74%，レーヨン56%，ポリエステル繊維77%であった。

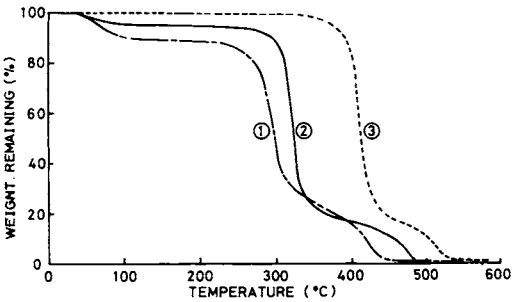

Fig. 9 Thermogravimetric curves in air flow (50ml/min.) 1. RAYON 2. CELLULOSE 3. POLYESTER FIBER

4. 考察

この研究では，火災時に生ずるような高温下におかれた高分子試料の熱分解による重量減少速度，とくにその最大値と試料温度との関係，および試料による差を知ることを目的とした。等温熱分解曲線にみられる最初の小さな重量減少の割合は，試料に含まれる水分の割合とよく一致している。したがって，この重量減少は，主として試料中の水分の蒸発によるものなのでこの部分の重量減少速度を無視する。

各試料を空気気流中で等温熱分解して得た最大重量減少速度の対数と加熱温度の逆数の関係は，**Fig.10**に示されるように，すべて直線となった。それぞれの直線から，加熱温度T（K）と最大重量減少速度（−dw/dt)max（mg／s）の関係を次の様に表わすことができる。

セルロース

$$\left(-\frac{dw}{dt}\right)_{max} = 3\times10^{4}\exp\left(-\frac{7.4\times10^{3}}{T}\right) \quad (1)$$

レーヨン

$$\left(-\frac{dw}{dt}\right)_{max} = 2\times10^{2}\exp\left(-\frac{5.4\times10^{3}}{T}\right) \quad (2)$$

ポリエステル繊維

$$\left(-\frac{dw}{dt}\right)_{max} = 2\times10^{6}\exp\left(-\frac{1.1\times10^{4}}{T}\right) \quad (3)$$

式（1）~（3）によれば，500 ℃以下ではレーヨンの最大重量減少速度がもっとも大きく，ポリエステル繊維で最小である。それぞれの試料の350 ℃における最大重量減少速度を求めると，セルロース0.2mg/s，

レーヨン 0.4mg/s, ポリエステル繊維0.02mg/ sとなりセルロース，レーヨンの分解が活発に起るこの温度においても，ポリエステル繊維はそれらに比べ，極めて安定である。このことは，仮に 350℃での一酸化炭素の試料重量当りの発生率がすべての試料で同一ならば，ポリエステル繊維からの一酸化炭素の発生速度は，350℃において，セルロースの1/10，レーヨンの1/20と考えられ，有毒ガスの発生による高分子材料の火災時の危険性を評価する上で，重量減少速度を考慮することの重要性が理解される。また，(1)～(3)式から，700℃以上で上記の重量減少速度の関係が逆転し，ポリエステル繊維の最大重量減少速度がもっとも大きくなることが予想される。

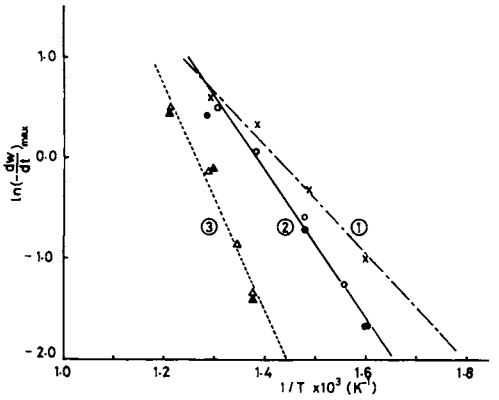

Fig. 10 ln $(-dw/dt)_{max}$ vs. 1/T plots.
1. RAYON 2. CELLULOSE 3. POLYESTER FIBER ○, △, ×: 21% O_2, ●, ▲: 15% O_2

昇温法により得られた熱重量曲線において，分解反応による第一段目の重量減少の割合が最大なので，重量減少速度にもっとも寄与していると考えられる。したがって，この部分についてBroido法[7]によりみかけの反応速度の解析を行った結果，各試料ともこの部分の分解量の10%より90%の範囲で反応次数1としてよい直線関係が得られ，活性化エネルギーE(Kcal/mol)と頻度因子A(s^{-1})として**Table 1**の結果を得た。ここで頻度因子はBroidoの近似$\exp(-E/RT) \fallingdotseq (Tm/T)^2\exp(-E/RT)$ のT_mとして，10%分解時の温度と90%分解時の温度との中点温度をとり見積った。ここにRは気体定数 (1.987Kcal/mol)，T_mは重量減少速度最大時の温度 (K) である。**Tabl 1** の結果は，各試料の第一段目の分解曲線をよく再現したが，ヘリウム中での同じ試料の熱分解から得られた活性化エネルギーと比較すると，レーヨンではほぼ同じ大きさであったが，ポリエステル繊維はヘリウム中で得られたものより約10 Kcal/mal，セルロースは約30 Kcal/molも大きかった。

Table 1 Overall Kinetic parameters of polymers obtained from the first stage decomposition in thermogravimetric analysis in air flow.
E: ACTIVATION ENERGY A: FREQUENCY FACTOR

POLYMER	E (Kcal/mol)	A (1/sec)
CELLULOSE	86	1.9×10^{29}
RAYON	41	1.7×10^{19}
POLYESTER	77	1.8×10^{22}

等温法および昇温法のいずれの熱分解においても，試料に含まれる水分は試料の分解開始以前か分解初期に蒸発しきる。また，等温熱分解の場合の分解量の割合は，加熱温度により残渣量が変化するけれども，セルロース約70%，レーヨン約65%，ポリエステル繊維約80%と昇温法により熱分解を行った場合の分解量の割合とよく一致している。ただし，等温法の場合の残渣量は**Figs. 6**～**8**の各線曲を外そうし，残重量軸との交点から求めた。以上の事実は，等温熱分解より求めた最大重量減少速度と比較できる重量減少速度を，昇温法による熱分解曲線から求めた**Table1**の結果を用いて求めることが可能であることを示している。

昇温法による熱重量曲線の解析を，反応次数を1として行ったので，基本となる速度式は

$$-\frac{dx}{dt} = kx \qquad (4)$$

ここで，$x = (w - w_\infty)/(w_0 - w_\infty)$

$k = A\exp(-E/RT)$

ただし，wは時間t(s)での試料の残重量(mg)，w_0は初めの試料重量，w_∞は残渣量である。(4)式に，これらの式を代入すると

$$\left(-\frac{dw}{dt}\right) = A\exp\left(-\frac{E}{RT}\right)(w - w_\infty) \qquad (5)$$

(5)式が最大重量減少速度を与えるのは，温度Tが一定ならwが最大のときである。したがって，試料の全量を50mgとして**Fig. 9**の縦軸を換算し，wとしてはそれぞれの試料の第一段目の分解による重量減少開始時の試料重量を，w_∞には残渣量をとり，**Table 1**のEとAとを用いれば，等温法による熱分解で得られた最

大重量減少速度と加熱温度との関係式（1）～（3）に対応する式が得られる。各試料について得られた結果は次のとおりである。

セルロース

$$\left(-\frac{dw}{dt}\right)_{max} = 7\times10^{30}\exp\left(-\frac{4.3\times10^4}{T}\right) \quad (6)$$

レーヨン

$$\left(-\frac{dw}{dt}\right)'_{max} = 5\times10^{14}\exp\left(-\frac{2.0\times10^4}{T}\right) \quad (7)$$

ポリエステル繊維

$$\left(-\frac{dw}{dt}\right)'_{max} = 7\times10^{23}\exp\left(-\frac{3.9\times10^4}{T}\right) \quad (8)$$

ただし，式（6）～（8）を式（1）～（3）と区別するためプライムを付けた。これらの式をそれぞれ試料ごとに比較すると，等温法により求めた最大重量減少速度の温度依存性は，昇温法により求めた結果に比較してきわめて小さく，しかも両者の間に特別な関係は認められないことがわかる。

秋田[8]は，種々の方法を用いて木材の分解の活性化エネルギーを広範な温度範囲で求めた結果，高温になるにつれ次第に小さくなる傾向を示し，400～470℃で18Kcal/mol，470～720℃で13Kcal/molであったと報告している。この程度の大きさの活性化エネルギーが，我々の等温熱分解による重量減少の最大値の温度依存を説明する。それゆえ，その温度依存性が，昇温法により得られたものより小さかった理由の一つは，昇温法における試料の分解温度範囲よりも高い温度域で等温法による測定がなされたためと考えられる。両方法により求めた最大重量減少速度の温度依存性の間に特別な関係が認められず，またそれらの大きさも異なったことは，火災時に生じるような高温下におかれた高分子物質の重量減少速度を，低い温度域で得られた活性化エネルギーにより見積ってはならないことを示している。

酸素濃度を21%より15%に減少させても，セルロース，ポリエステル繊維の等温熱分解による重量減少の様子に変化がなかった。酸素濃度15%の空気気流中で行った等温熱分解から得られた最大重量減少速度の対数と加熱温度の逆数の関係も**Fig.10**に示した。この関係も酸素濃度21%と大差ない。したがって，試料温度を一定に保った熱分解においては，この程度の酸素濃度の変化は試料の熱分解に大きな影響を与えないと考えてよい。

我々のセルロースについての等温熱分解による重量減少の様子は，**Fig. 6** にみられるように重量減少速度（−dw/dt）と残重量wとの関係において放物線状となるものであり，秋田[8]の減圧下（2 Torr）での等温熱分解やLipskaら[9]の窒素気流中での等温熱分解の結果と異なった。この原因についてはさらに検討が必要である。

この研究を行うに当り，終始御助言，御指導下さった横浜国立大学工学部上原陽一助教授および装置の試作，改良に御協力下さった当研究所宮田作技官に，心から感謝する。

参考文献

1) 炭谷孝一：火災科学セミナーテキスト，P49，日本火災学会（1974）
2) J.P.Wagner：Fire Reserch Abstruct and Review，**14**，1（1972），（日本語訳）上原陽一：安全工学，**13**，322（1974）
3) 土屋能男：火災，**25**，3（1975）　**25**
4) 斉藤文春：日本火災学会論文集，**18**，（No.2），9（1968）
5) 牧　廣：化学と工学，**24**，1035（1971）
6) K.Sumi and Y.Tsuchiya：J.Combustion Toxicology，**2**，213（1975）
7) A.Broido：J.Polymer Sci.，**7**，1761（1961）
8) 秋田一雄：消防研究所報告，**9**，1（1959）
9) A.E.Lipska and W.J.Parker：J.Appl. Palymer Sci.，**10**，1439（1996）

Weight Loss Rates of Polymers Pyrolyzed Isothermally at High Temperature in Air Flow (Part 1. Cellulose, Rayon and Polyester Fiber)

(Abstract)

Naoshi Saito and Eiji Yanai

(Recieved May 31, 1976)

The isothermal pyrolysis of cellulose, rayon and polyester fiber was carried out in air flow in the temperature range 350–550°C, and the weight loss rates were measured. With every polymer used, it is shown that the logarithm of maximum weight loss rate decreases linearly with the increase in the reciprocal of absolute temperature. At temperatures below 500°C, rayon shows the largest value in the maximum weight loss rate, while polyester fiber the smallest. On the other hand, it is estimated that the above relation is reversed at temperatures above 700°C. With every polymer used, the temperature dependence of the maximum weight loss rate is smaller than expected from the first stage of decomposition in the thermogravimetric analysis in air flow. Reduction of oxygen concentration from 21% to 15% has no influence on the weight loss with cellulose and polyester fiver.

建物内の煙の流動
（その1）　非定常状態における水平二層流の略算法による計算及び実験

（概　　要）

佐藤晃由

（昭和51年6月3日受理）

建物火災時の在居者の避難と救助に関する対策を煙の流動性状に基づいて検討する際，現状では煙の流動予測法として非定常略算法が用いられているが，その場合，計算と実験との間にはどの程度の差異が存在するかについての報告は少ない。このような見地から，筆者は廊下内での煙の流動を一つのモデル・ケースと考え，水平二層流に関する実験と計算との比較を行なうことを試みた。

その結果，両者は大体においては一致し，火災初期における廊下内での煙の流動性状はこの計算法により，予測できることが知られた。しかしながら，諸々の影響から温度に関する計算値と実験値の間に2割程度の差を生じた。これは計算モデルの修正，実験方法の改良により縮小させうるものと思われる。

Smoke Movement in A Building (Part 1 The calculation with Approximate Calculation Method and the experiment on the smoke-air stratified flow in the unsteady state)

Kohyu Satoh

(Received June 3, 1976)

In order to investigate the effective evacuating plan for the occupants of a building in fire, it is important to predict the smoke movement in the building. For this purpose, Approximate Calculation Method is generally used in Japan. However, there have been few reports concerning the experimental verification of the calculative results, especially with the smoke-air flow in the unsteady state. Accordingly, an attempt was made to compare the calculation and the experiment on the smoke-air flow in a corridor, as a typical case.

The results show that the calculation agrees on the whole with the experiment and therefore the smoke movement in a corridor may well be predicted with this calculation method.

1. Introduction

A great volume of smoke produced during fires prevents occupants in buildings from escaping or being rescued. Therefore, it is important to predict the smoke movement not only for designing safe buildings to be constructed hereafter, but also in order to investigate the effective counterplan for evacuating the occupants during fires in the present buildings. The author's purpose is to find a reasonable indication for actions of fire brigades and for designing a reliable emergency guiding system[1] for occupants, based on the prediction of the smoke movement.

There are two ways as calculation method to predict the smoke movement in buildings in the unsteady state. One is Approximate Calculation Method[2] introduced by the group of BRI (the Building Research Institute of Japan) and another is an orthodox method by the group of UND (the University of Notre Dame)[3], using cell model and based on some physical or fluid dynamical governing equations. At present, the former is generally used in Japan. In order to predict the smoke movement, it is necessary to have a knowledge about the difference between the calculation and the experiment on the smoke-air flow in the unsteady state. Nevertheless, there have been few reports on this matter, except some literatures[4),5] referring mainly to the calculation. The author paid attention to this point and made the calculation and the experiment using a part of the test building in the Fire Research Institute.

On the steady state smoke spreading, there have been a few reports[6),7] which pertains to a comparison of the experiment with the calculation, using Approximate Calculation Method. However, no comprehensive measurements on all unknowns contained in the equations have

been made in them. For example, no or only fragmental measurements have been made on the air velocity and the height of neutral plane. An attempt should be made to compare the calculation and the experiment not only on partial unknowns, but also on all the other unknowns appearing in the simultaneous equations.

He, therefore, made an attempt in this study to measure all the unknowns in the unsteady state, such as temperature, air velocity, height of neutral plane and boundary layer, and pressure difference, and compare them with the calculative results.

Nomenclature

Q_{nm} (m>n) : hot outflow through the n-th opening from the n-th block to the m-th block (kg/s). (Suffix n, m; number of block)

Q_{mn} (m>n) : cold inflow through the n-th opening from the m-th block to the n-th block (kg/s).

Y_n : height of neutral plane at the n-th opening (m).

X_n : height of hot-cold air boundary layer in the n-th block (m).

α : coefficient of opening (α=0.7).

B_n : width of the n-th opening (m).

H_n : height of the n-th opening (m).

HL_n : bottom height of the n-th opening (m).

γ_n : hot air density in the n-th block (kg/m^3).

γ_O : density of outside cold air (kg/m^3).

P_{n-m} : pressure difference at the floor level between block n and block m (kg/m^2).

g : gravitational acceleration (9.8m/s^2).

2. Experimental

1) *Experimental method*

The experiment was performed in a corridor of the test building as illustrated in Fig. 1 This corridor has a length of 20m, a width of 1.24m and a height of 2.5m. One end of the corridor is closed and the opposite end is opened to the outer air. Four tarekabes (hanging walls) were set beneath the ceiling of the corridor (see Fig. 1), and so the corridor was divided into four

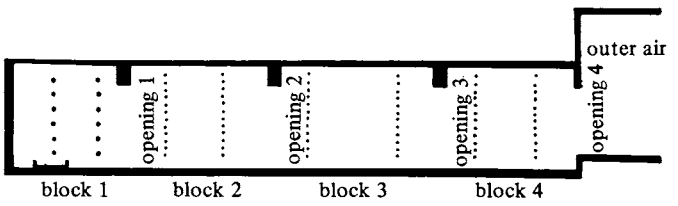

Fig. 1 Schematic diagram of the corridor used in the experiment. Dots denote the points where thermocuples were set. The sign on the floor in the block 1 depicts the fuel vessel.

Table 1. Dimensions of the corridor.
The figures are given in meters.

	Block 1	Block 2	Block 3	Block 4
Height of opening	1.9	2.1	2.2	2.4
Width of opening	0.72	0.89	1.17	1.78
Length of block	2.3	5.0	5.3	4.2
Width of block	1.24	1.24	1.24	1.24
Length of tarekabe	0.6	0.4	0.3	0.26
Height of bottom opening	0.0	0.0	0.0	0.26

blocks by them. The reason for dividing into four blocks will later be referred in section 3. The dimensions of these blocks are shown in Table 1. Block 1 was designated burn room and a square fire tube, 90cm x 90cm and 10cm in depth, was placed on the floor. In every run, 15 liters of methanol were poured into the tub and ignited.

Methanol was preferred as the fuel because: (1) a liquid fuel was favourable as compared to a solid fuel for securing the reproducibility of phenomena in the initial burning stage, and (2) its soot-free burning could avoid the difficulty in air velocity measurements due to the adhesion of soots on the sensors of hot-wire anemometers.

The quantities measured after ignition were:(1) temperature increase in each block, (2) air velocity at each opening, (3) height of neutral plane at each opening and smoke layer in each block, and (4) pressure difference at the floor level between the blocks. Measurements were carried on by repeating the same runs with varying the measured points, for lack of measuring instruments.

The temperature in each block was measured with chromel-alumel thermocouples, having a diameter of 0.32mm. These were set on 6 points vertically in block 1 and 12 points in other blocks, and two places horizontally in each block. The air velocities were measured with two hot-wire anemometers, one for high temperature and another for low temperature, and also with pitot-tubes combined with very sensitive differential manometers. Such manometers were also used for measuring the pressure difference. Heights of neutral planes and the bottom of hot air were measured visually by flow of smoke produced by joss sticks.

2) *Results of experiment*

Temperatures in each block are shown in Figs. 2 and 3. Each curve was obtained through the mean of temperatures at two places of the same level, except points 5 and 6 in block 1. However, the remarkable difference was not observed between those two temperatures. Numerals by the curves indicate the measured points. Mean temperature in the fire room is the arithmetical mean for points 1 to 5. Points 6 and 6', vertically the lowest, were at the same level. Point 6' was within the flame of fire, while 6 was outside the flame. The reasons for exclusion of points 6 and 6' in averaging the temperatures in block 1 were:(1) the bottom of very hot air lay between the points 5 and 6, and (2) the point 6' was within the flame and the very high temperature there, if included in the arithmetical mean, therefore would make the mean temperature in block 1 excessively high.

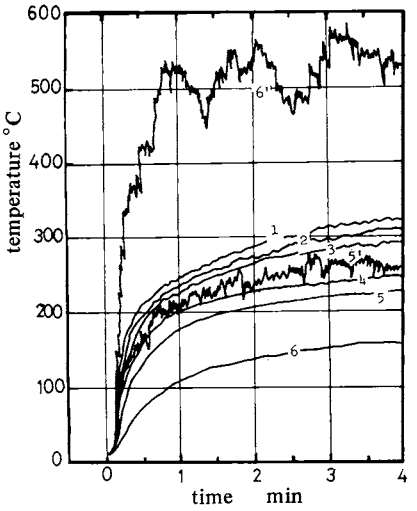

Fig. 2 Temperatures in the block 1 as a function of time given from ignition. Numerals show the heights of the measured points, as follows. 1 ; 2.33m 2 ; 1.96m 3 ; 1.58m 1 ; 2.33m 2 ; 1.96m 3 ; 1.58m 4 ; 1.20m 5 and 5' ; 0.83m 6 and 6' ; 0.41m (5 and 5', 6 and 6' were at the same height respectively, but 5' and 6' were in the flame of fire.)

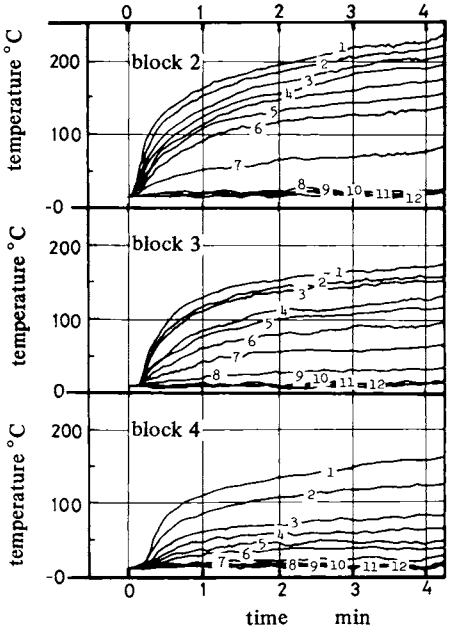

Fig. 3 Temperatures in the block 2, 3 and 4 as a function of time given from ignition. Numerals show the heights of the measured points, as follows. 1; 2.36m 2; 2.15m 3; 1.95m 4; 1.78m 5; 1.60m 6; 1.43m 7; 1.25m 8; 1.06m 9; 0.85m 10; 0.60m 11; 0.40m 12; 0.20m

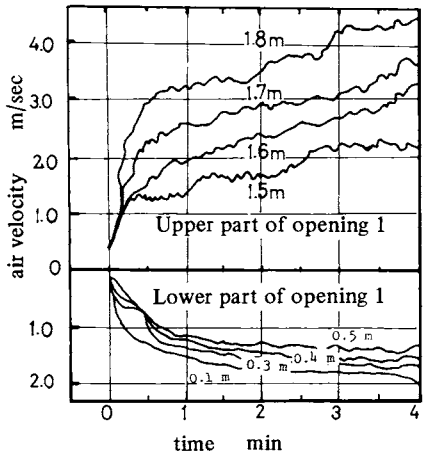

Fig. 4 The relations of air velocities at the opening 1 vs. time after ignition. The numerals in the figure show the heights of the measured points.

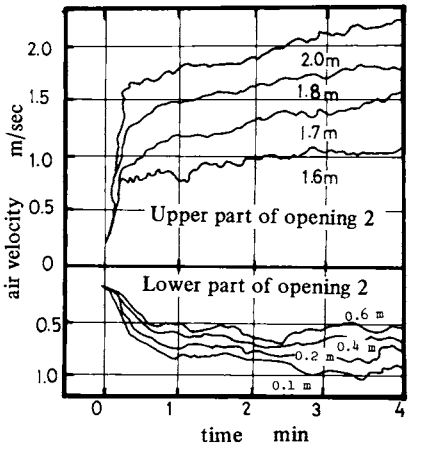

Fig. 5 The relations of air velocities at the opening 2 vs. time after ignition. Numerals are the same as in Fig. 4.

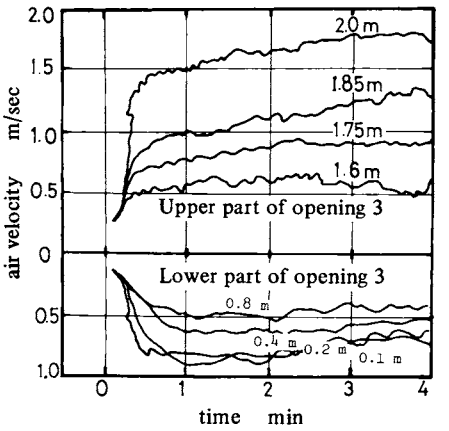

Fig. 6 The relations of air velocities at the opening 3 vs. time after ignition. Numerals are the same as in Fig. 4.

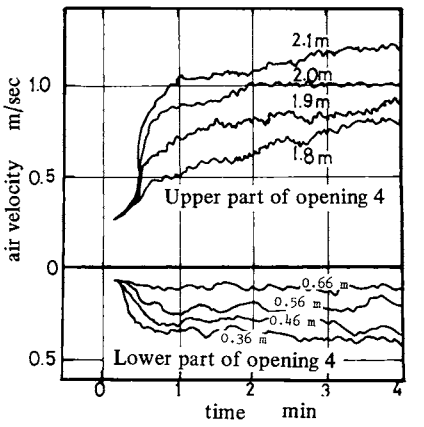

Fig. 7 The relations of air velocities at the opening 4 vs. time after ignition. Numerals are the same as in Fig. 4.

This mean temperature was used as input data in computing. Mean temperature of hot air in the second block is the arithmetical mean for points 1 to 8, in the third block for point 1 to 7 and in the fourth block for points 1 to 6.

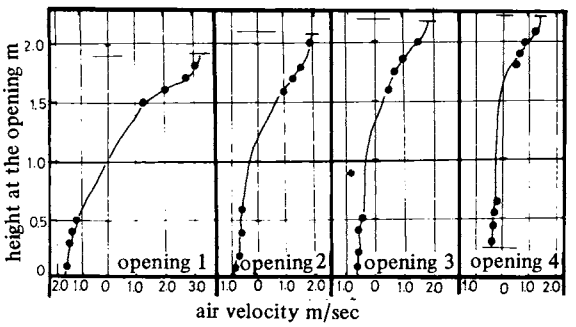

Fig. 8 Relationship between air velocity at the time of 1 minute given from ignition and the height at the opening.

Air velocities measured are shown in Figs. 4 to 7. Fig. 8 shows the relationship between the air velocity and the height at each opening at the time of 1 minute after ignition. Fig. 9 shows the pressure difference between blocks 1 and 4, and that between blocks 2 and 4.

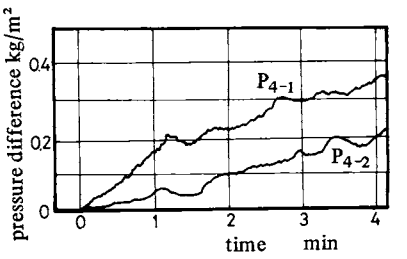

Fig. 9 The relations of pressure difference vs. time given from ignition. P_{4-1}; pressure difference at the floor level between block 1 and block 4. P_{4-2}; pressure difference at the floor level between block 2 and block 4.

The height to the bottom of hot layer in block 2 was about 1.1m, in block 3 about 1.3m and in block 4 about 1.5m. The height of neutral plane was about 1.0m at opening 1, about 1.2m at opening 2, about 1.4m at opening 3, and about 1.6m at opening 4, at the time of 1 minute after ignition.

3. Calculation

1) *Calculation procedure*

The procedure to analyze smoke movement in a building in the unsteady state is as follows: (1) dividing a building into some optional blocks, (2) giving dimensions of each block, (3) giving initial temperature of each block, (4) setting time forward by Δt, a definite interval of time, (5) giving temperature increase in the first block, i.e., fire room*, (6) calculating inflows and outflows through openings of each block, (7) calculating the sum of inflows from the adjacent block, (8) judging whether smoke overlows from this block to the next block, (9) calculating inflows and outflows through opening if smoke overflows, (10) calculating temperature of smoke in the block, (11) advancing further to the next block with the same procedure, and (12) repeating above procedures with setting time forward by Δt.

2) *Calculation model*

A corridor of a building was selected as a typical model and divided into four blocks by four tarekabes. These were based on the following reason: (1) it is difficult to make measurements if the scale of a model is too extensive, (2) temperature differences between blocks should exist, and (3) temperature gradient in a room will be too steep if the room is too extensive.

In case of this model, the hot and cold air flows will form a stratified counterflow. The stability of this interesting stratified flow has been reported by the group of the University of Kyoto[8] through a small model experiment.

Two types, A and B, of profile of pressure difference are illustrated in Fig. 10. Either of

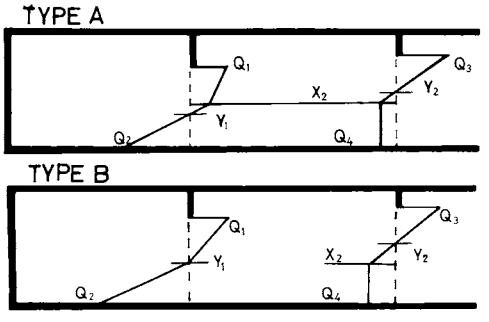

Fig. 10 Profiles of the pressure difference.
Type A; in case of this profile, the outflow and inflow at the i-th opening and the i+l-th opening are strongly affected by the height of smoke layer (X_{i+1}).
Type B; In case of this profile, the outflow and inflow at the i-th opening are not affected by the height of smoke layer (X_{i+1}), but they are affected by only X_i.

them is used as a calculation model to analyze such a stratified flow. With the case of type A, the outflow at the i-th opening is affected by the height of the bottom of hot air in the i+1-th block, while with type B, it is not. In some cases, it was impossible to solve the equations, using

* Generally, temperature increase in the fire room should be calculated from heat generation, but in this report experimental values were used.

the type A. Using the type B, the equations could be solved and therefore the type B was selected as a calculation model.

The variation of the profile of pressure difference in the corridor with the lapse of time after ignition is depicted in Fig. 11 (A to D).

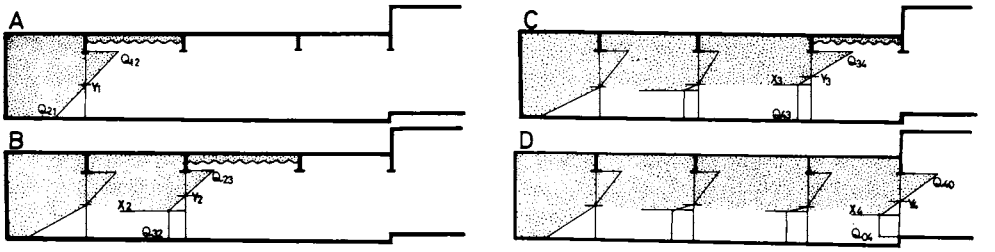

Fig. 11 Variation of the profile of pressure difference with the lapse of time given from ignition.

A; Until the hot air overflows the 2-nd tarekabe.
B; Until the hot air overflows the 3-rd tarekabe.
C; Until the hot air overflows the 4-th tarekabe.
D; After the hot air overflows the 4-th tarekabe.

3) *Equations for calculation*

Unknown quantities can be calculated by the following equations.

$$Q_{12} = \frac{2}{3}\alpha B_1\sqrt{2g\gamma_1(\gamma_2-\gamma_1)}\,(H_1-Y_1)^{1.5} \quad \ldots\ldots(1)$$

$$Q_{21} = \frac{2}{3}\alpha B_1\sqrt{2g\gamma_0(\gamma_0-\gamma_1)}\,Y_1^{1.5} \quad \ldots\ldots(2)$$

$$Q_{23} = \frac{2}{3}\alpha B_2\sqrt{2g\gamma_2(\gamma_3-\gamma_2)}\,(H_2-Y_2)^{1.5} \quad \ldots\ldots(3)$$

$$Q_{32} = \frac{1}{3}\alpha B_2\sqrt{2g\gamma_0(\gamma_0-\gamma_2)(Y_2-X_2)}\,(2Y_2+X_2) \quad \ldots\ldots(4)$$

$$Q_{34} = \frac{2}{3}\alpha B_3\sqrt{2g\gamma_3(\gamma_4-\gamma_3)}\,(H_3-Y_3)^{1.5} \quad \ldots\ldots(5)$$

$$Q_{43} = \frac{1}{3}\alpha B_3\sqrt{2g\gamma(\gamma_0-\gamma_3)(Y_3-X_3)}\,(2Y_3+X_3) \quad \ldots\ldots(6)$$

$$Q_{40} = \frac{2}{3}\alpha B_4\sqrt{2g\gamma_4(\gamma_0-\gamma_4)}\,(H_4-Y_4)^{1.5} \quad \ldots\ldots(7)$$

$$Q_{04} = \frac{1}{3}\alpha B_4\sqrt{2g\gamma_0(\gamma_0-\gamma_4)(Y_4-X_4)}\,(2Y_4+X_4-3HL_4) \quad \ldots\ldots(8)$$

$$Q_{12} = Q_{21} \quad \ldots\ldots(9) \qquad Q_{23} = Q_{32} \quad \ldots\ldots(10) \qquad Q_{34} = Q_{43} \quad \ldots\ldots(11)$$

$$Q_{40} = Q_{04} \ldots\ldots (12) \qquad Q_{12} = Q_{23} \ldots\ldots (13) \qquad Q_{23} = Q_{34} \ldots\ldots (14)$$

$$Q_{34} = Q_{40} \ldots\ldots (15)$$

$$P_{4\text{-}1} = (\gamma_0 - \gamma_1)\, Y_1 + (\gamma_0 - \gamma_2)\, (Y_2 - X_2) + (\gamma_0 - \gamma_3)\, (Y_3 - X_3) \ldots\ldots (16)$$

$$P_{4\text{-}2} = (\gamma_0 - \gamma_2)\, (Y_2 - X_2) + (\gamma_0 - \gamma_3)\, (Y_3 - X_3) \ldots\ldots (17)$$

Equation $Q_{n,n+1} = Q_{n+1,n+2}$ should be used, but there was a case where the equations could not be solved due to $Q_{n,n+1} > Q_{n+1,n+2}$, for the temperature difference between the n-th block and the n+1-th block was highly greater than that between the n+1-th block and the n+2-th block. In such a case, an adaptation was made by placing $Q_{n+1,n+2} = 0.95\, Q_{n,n+1}$. It was assumed that 5% of $Q_{n,n+1}$ mixed with lower cold air.

Temperature increase of hot air in each block, ΔT, was calculated by the following equation.

$$\Delta T = [QQ(\text{in}) - QQ(\text{out}) - QQ(\text{loss})] / (C_p\, \gamma\, V)$$

Where QQ(in) is the heat contained in inflowing air (k cal), QQ(out) the heat contained in outflowing air (k cal), QQ(loss) the heat loss to walls and ceiling (k cal), C_p the specific heat of air at constant pressure (0.238 kcal/kg.deg), γ the mean density of hot air (kg/m^3), and V the volume of hot layer (m^3). QQ(loss) was calculated by the method shown in ref. 2.

Unknown quantities are as follows:

Q_{12}	Q_{21}	Q_{23}	Q_{32}	Q_{34}	Q_{43}	Q_{40}	Q_{04}	
Y_1	Y_2	Y_3	Y_4	X_2	X_3	X_4	$P_{4\text{-}1}$	$P_{4\text{-}2}$

4) *Results of calculation*

The calculation was performed by the aid of DEMOS-E, a TSS computing system.

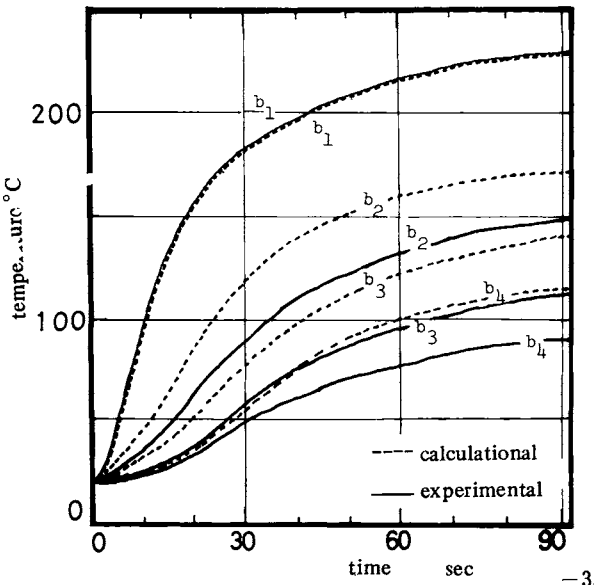

It was frequently impossible to perform the calculation, for it was impossible to make Q_{12} equal to Q_{23} and Q_{23} equal to Q_{32} after starting from Q_{12} equal to Q_{21}. Therefore, the calculation model was modified, little by little.

In Fig. 12, temperatures calculated are given in dotted lines and mean temperatures obtained from the experiment in solid lines.

Fig. 12 Relationship between mean temperature of hot air in the upper part of each block and time given from ignition. b_i; block i (i =1, 2, 3, 4)

The other calculated quantities are shown in Table 2. Although the calculation was performed at intervals of two seconds, only partial results were given here.

Table 2. Results of the calculation given from equations (1) to (17). The calculation was performed at intervals of 2 seconds, but partial results were given here. (Time was given from ignition.)

time	Q_{12}	Y_1	Q_{23}	Y_2	X_2	Q_{34}	Y_3	X_3	Q_{40}	Y_4	X_4	P_{4-1}	P_{4-2}
sec	kg/sec	m	kg/sec	m	m	kg/sec	m	m	kg/sec	m	m	kg/m²	kg/m²
2	0.20	0.95	0.00	0.00	0.00	0.00	0.00	0.00	0.00	0.00	0.00	0.02	0.00
8	0.58	0.86	0.53	1.12	0.70	0.00	0.00	0.00	0.00	0.00	0.00	0.20	0.03
12	0.70	0.84	0.60	0.89	0.09	0.54	1.30	1.10	0.00	0.00	0.00	0.36	0.11
14	0.72	0.83	0.69	0.97	0.44	0.65	1.14	0.77	0.59	1.35	1.04	0.39	0.11
20	0.71	0.77	0.67	1.08	0.88	0.64	1.22	1.07	0.61	1.54	1.45	0.38	0.07
30	0.64	0.69	0.61	1.11	1.01	0.58	1.32	1.26	0.55	1.72	1.69	0.36	0.05
50	0.58	0.63	0.55	1.03	0.95	0.53	1.25	1.21	0.50	1.82	1.81	0.35	0.04
80	0.56	0.61	0.54	0.99	0.91	0.51	1.14	1.10	0.48	1.84	1.83	0.36	0.05
120	0.56	0.60	0.53	0.98	0.90	0.51	1.11	1.07	0.48	1.85	1.84	0.37	0.05
170	0.56	0.60	0.54	0.98	0.90	0.51	1.11	1.07	0.48	1.85	1.84	0.38	0.05

4. Discussion and conclusion

The results show that the calculation agrees with the experiment on the whole, but temperature increases in the calculation were larger than in the experiment. Radiation might have affected the measurement of the temperature in block 1. If the mean temperature in block 1 is reduced a little, the temperatures calculated for other blocks would be in better accord with the experimental results.

From Fig. 8, the mass flow rates of air through the openings are obtained as follows:

$Y_1 = 1.0\text{m}$ $\quad Q_{12} = 0.69\text{m}^3/\text{s} = 0.50\text{kg/s}$ $\quad (\gamma_1 = 0.72\text{kg/m}^3)$

$\quad Q_{21} = 0.44\text{m}^3/\text{s} = 0.54\text{kg/s}$ $\quad (\gamma_0 = 1.23\text{kg/m}^3)$

$Y_2 = 1.2\text{m}$ $\quad Q_{23} = 0.59\text{m}^3/\text{s} = 0.52\text{kg/s}$ $\quad (\gamma_2 = 0.88\text{kg/m}^3)$

$\quad Q_{32} = 0.30\text{m}^3/\text{s} = 0.37\text{kg/s}$ $\quad (\gamma_0 = 1.23\text{kg/m}^3)$

$Y_3 = 1.4\text{m}$ $\quad Q_{34} = 0.56\text{m}^3/\text{s} = 0.53\text{kg/s}$ $\quad (\gamma_3 = 0.96\text{kg/m}^3)$

$\quad Q_{43} = 0.43\text{m}^3/\text{s} = 0.53\text{kg/s}$ $\quad (\gamma_0 = 1.23\text{kg/m}^3)$

$Y_4 = 1.6\text{m}$ $\quad Q_{40} = 0.49\text{m}^3/\text{s} = 0.49\text{kg/s}$ $\quad (\gamma_4 = 1.00\text{kg/m}^3)$

$\quad Q_{04} = 0.40\text{m}^3/\text{s} = 0.49\text{kg/s}$ $\quad (\gamma_0 = 1.23\text{kg/m}^3)$

These mass flow rates are in accord with the results of calculation, but the heights of the bottom of hot air and neutral plane are not in accord with the results of calculation in Table 2.

As shown in Fig. 9 and Table 2, the calculated pressure difference is in accord with the result of experiment for P_{4-1}, but not for P_{4-2}. The model for calculation may be necessary to be modified. As mentioned above, with some quantities, there exist noticeable differences between calculation and experiment, whereas some may be in accord, but on the whole the calculation can predict the movement of smoke. The author and his colleagues are going to investigate the effective counterplan for evacuating the occupants in buildings by the aid of this

calculation method, modifying the model for calculation.

5. Acknowledgement

The author would like to thank his colleagues and Mr. Y. Kumano, the Director of the Fire Research Institute, for helpful suggestions and for permission to publish this paper.

6. References

1) Y. Yamada: Electric engineering magazine OHM, December, p.57, (1975).
2) Kenchiku Setsubi Sogokyokai: Devices for Fire Protection, Smoke Extraction and Fire Fighting in Buildings, p.113, OHM, (1975).
3) K.T. Yang, J.R. Lloyd, M.L. Doria: Fire Smoke Spread, NSF GRANT, GI-37191 ATA73-07749-A01, (1975).
4) T. Wakamatsu, T. Tanaka, K. Mogami, T. Yamana: Report of Special Researches on Prevention of Fire and Smoke Hazards in High-Rise and Complexed Buildings, p.143, Research Coordination Bureau of Science and Technology Agency, (1974).
5) P. Lieberman, D. Bell (TRW Systems Group): Fire Technology, Vol.9, No.2, p.91, (1973).
6) T. Jin, H. Shimada, A. Takemoto: Report of Fire Research Institute of Japan, No.40, p.35, (1975).
7) T. Wakamatsu: Occasional Report of Japanese Association of Fire science and Engineering, No.1, p.212, (1974).
8) T. Terai, K. Nitta: ibid, p.180.

消防研究所報告

通巻 42 号

昭和51年 9 月30日発行

編集
発行　自治省　消防庁　消防研究所

〒181　東京都三鷹市中原 3 丁目14番 1 号
電　話（0422）44－8331（代表）